Supporting Information

Graphene Oxide as a Nanocarrier for Controlled Delivery of Indole

Yasin Sadeghipour[1], Salar Hafez Ghoran[1,2]*, Mostafa Shafiee[1], Seyed AmirHossein Mousavi[1], Fatemeh Sadat Dehghani[1], Ali Mohammad Amani[1]*

1. *Department of Medical Nanotechnology, School of Advanced Medical Sciences and Technologies, Shiraz University of Medical Sciences, Shiraz, Iran.*
2. *Department of Chemistry, Faculty of Science, Golestan University, Gorgan, Iran.*

*Corresponding author:

***Salar Hafez Ghoran** (Department of Chemistry, Faculty of Science, Golestan University, Gorgan, Iran).

Phone number: +98-9144425047

Email address: S_Hafezghoran@yahoo.com

Abstract

Regarding the specific physiochemical and biomedical properties of graphene oxide (GO), it has been a long time that experts have preferred anticancer drug cocktails to single drugs. Given that the former may develop a more balanced molecular basis for recent chemotherapeutic strategies. In this study, graphene oxide was investigated as a bioavailable nanocarrier for indoles. The synthesized components were characterized using Fourier transform infrared (FTIR), X-ray diffraction (XRD), UV–Vis spectroscopies, and scanning electron microscopy (FE-SEM) techniques. Interestingly, maximum drug loading efficiency was achieved in the neutral media (pH=7). The release analysis in different media revealed higher rate in both acidic and basic media than in neutral media. However, the total loaded drug was released in less than 80 minutes in all the systems prepared. The MTT assay results toward mesenchymal stem cells exhibited a desirable biocompatibility of GO-indole and GO. Taken together, the prepared GO-indole has suitable drug loading efficiency.

Keywords: Bioavailability, Cancer, Drug delivery, Graphene oxide, Nanocarrier, pH sensitive.

Materials

Graphite flakes with -100 meshes, dimethyl sulfoxide (DMSO), potassium nitrate (KNO_3), sulphuric acid (H_2SO_4, 98%), potassium permanganate ($KMnO_4$), hydrochloric acid (HCl, 37%), and indole (molecular formula C_8H_7N, molecular weight 117.15 g/mol) were commercially purchased from Merck (Germany) and applied without further purification. Deionized water was used in all experiment.

Synthesis of Graphene Oxide

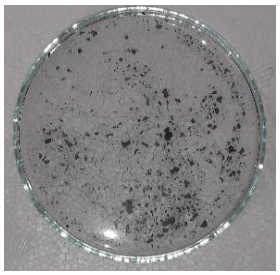

Figure S1: A nanoparticle synthesized on glass after being centrifuged.

Powder X-ray diffraction (XRD) analysis

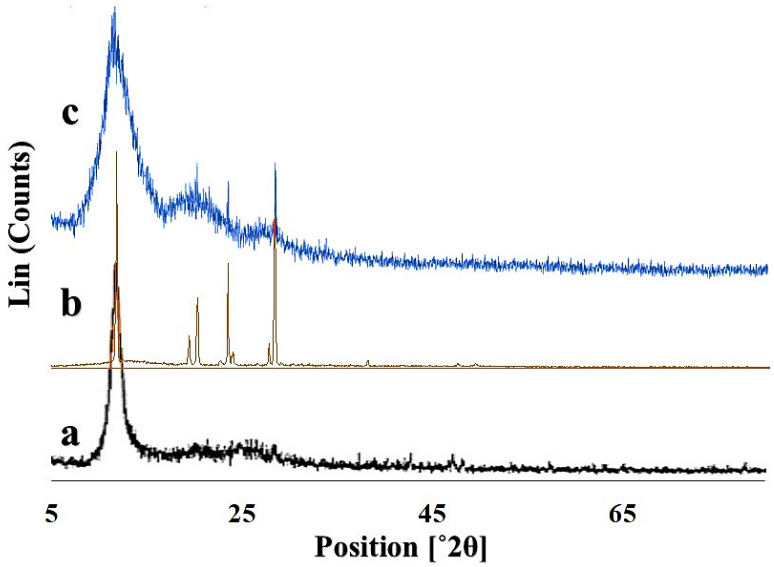

Figure S2: The X-ray diffraction patterns of **a**) GO, **b**) indole, and **c**) GO-indole nanoparticles.

Loading and release amount of indole from nanocomposite

The standard curve for the drug concentration versus ultraviolet absorption

In the present study, the ultraviolet spectrophotometry was applied to evaluate the drug loading and drug release over time. To do so, the absorption rate at the wavelength range of

200-800 nm was obtained to determine the peak characteristic of the material. The drug solution was prepared at different certain concentrations, and a standard curve was drawn for the drug absorption versus concentration. The drug release rate was predicted using the fitting equation. The maximum absorption wavelength of indole is 286 nm, which was used to characterize the indole in the environment of this study. To achieve the standard UV-absorption-concentration curve, the indole solution was first prepared with phosphate buffer of pH 7, according to Table S1. The UV absorbance of the solution was measured at the specific wavelength of 286 nm. The absorption versus drug concentration curve was then plotted, and the relationship between variables was fitted. Table S1 and Figure S3 show different concentrations of indole solution with their corresponding adsorption rate.

Table S1: Concentrations of the drug solution (mol/L) and their corresponding absorbance values at the wavelength of 286 nm.

Concentration (mol/L)	0	0.02	0.04	0.06	0.08	0.1	0.15
UV absorption rate	0	0.12	0.2	0.29	0.41	0.48	0.73

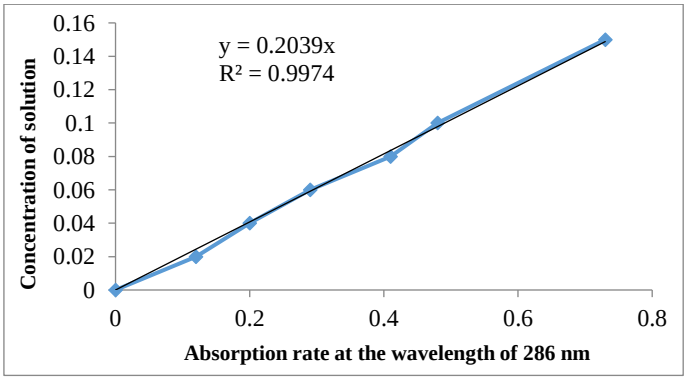

Figure S3. Standard curve of the indole solution.

As shown in Figure S2, the variables have been fitted accurately. The drug concentration in the solution was determined through measuring the amount of solution absorbed by the UV and using the following fitted equation:

$$C = 0.2039\lambda_{286}$$

Where, C is the molar concentration of indole solution (mol/L), and λ_{286} is the UV absorption of indole solution at the wavelength of 286 nm. To ensure that the solution pH did not affect the UV absorption, indole solutions of equal concentrations were prepared in phosphate buffer with different pHs. The absorbance of the solution was read at the wavelength of 286 nm. The results showed that the pH of the solution had no effect on the UV absorption of the solution.

Identifying the efficiency of drug loading

The standard UV absorption curve for the drug concentration and fitting curve were used to calculate the quantity and efficiency of drug loading.

$$Drug\ loading(\%) = \frac{M_{drug}}{M_{system}} \times 100 = \left(\frac{(C_0 - C_r) \times V \times M_{indole}}{(C_0 - C_r) \times V \times M_{indole} + M_{graphene\ oxide}}\right) \times 100$$

$$Drug\ loading\ efficiency(\%) = \left(1 - \frac{C_r}{C_0}\right) \times 100 = \left(1 - \frac{\lambda_r}{\lambda_0}\right) \times 100$$

Drug delivery with adaptation of soluble concentrations

In this study, Langmuir adsorption isotherm was used to evaluate adsorption capability and changes in the adsorption capacity of GO at different pHs. The Langmuir equation is shown below:

$$\frac{C_e}{q_e} = \frac{C_e}{q_{max}} + \frac{1}{bq_{max}}$$

Adaptation of *in vitro* drug release pattern with semi-experimental models of drug release

In the present study, the release of Indole from graphene nanocomposite was evaluated using pseudo–first order (Equation 1), pseudo–second order (Equation 2) and Korsmeyer–Peppas (equation 3) models as follows:

Equation 1: $$\ln\left(\frac{q_e - q_t}{q_e}\right) = -kt$$

Equation 2: $$\frac{t}{q_t} = \frac{1}{kq_e^2} + \frac{t}{q_e}$$

Equation 3: $$\frac{M_t}{M_\infty} = kt^n$$

System stability at ambient temperature

Given that the quality of the drug release system must be kept during the storage of the nanoparticles, the nanomaterials were stored in a container at the room temperature. Similar to the previous drug release section, a certain amount of the nanomaterials was added to their release medium after 1-60 days, and the release analysis was repeated.

Toxicity and biocompatibility of samples

The MTT test was performed to examine the toxicity and compatibility of the system. In summary, Human mesenchymal stem cells (hMSCs) were cultured in a 96-well plate of a density of 20,000 cells/cm^2. After 24 hours, the extracellular culture medium and 200 µl of the test medium were added to the wells. The samples were then incubated in a cell culture medium at 37 °C and 5% carbon dioxide for 48 hours. In a dark environment, the culture medium was removed and replaced with 200 µl of MTT colored solution in a cell culture medium buffer. After 3 hours of heating, the colored solution was removed, and 200 µl of dimethyl sulfoxide was added to the solution. Having used ELISA reader, the absorbance was read at the wavelength of 570 nm and compared with the absorbance of the control solution. The following

equation was used to calculate the percentage of cell viability.

$$Cell\ viability(\%) = \frac{I_c}{I_{c^-}}$$

Efficiency and quantity of indole loading

The amount of drug absorbed on GO reached maximum at the neutral pH probably due to the free paired-electron on the nitrogen atom in the indole drug, which could easily form a hydrogen bond with GO. At acidic pHs, however, the surface of indole's nitrogen becomes positive because of protonation. At basic pHs, the surface of indole's nitrogen is deprotonated, and the tendency to bind with the functional group on GO surface gets lower due to the involvement of the free paired electrons. The optimal pH for loading the drug should be therefore neutral (Figure S4).

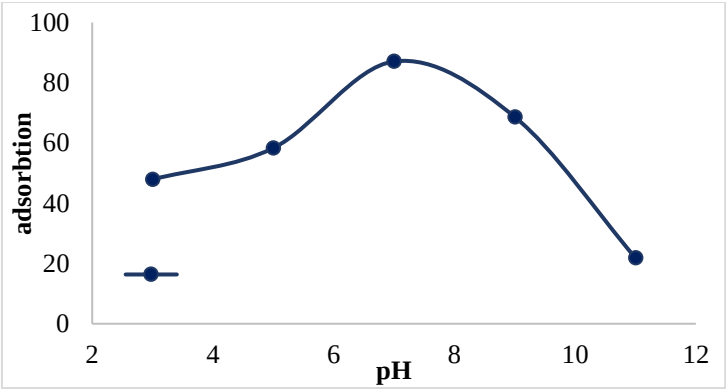

Figure S4. The amount of loaded indole onto graphene oxide at different pHs.

Table S2: Loading the indole onto graphene oxide at different concentrations of indole and pH 3.

Item	Primary drug concentration (mol/L)	Primary UV absorption of drug solution (λ)	Final UV absorption of drug solution (λ)	Drug loading efficiency (%)	Quantity of drug loading (%)
1	0	0	0	0.00	0
2	0.02	0.12	0	100.00	48.38
3	0.04	0.2	0	100.00	65.21
4	0.06	0.29	0.10	65.52	64.99
5	0.08	0.41	0.18	56.10	66.99
6	0.10	0.48	0.25	47.92	69.67
7	0.15	0.73	0.39	46.58	76.76

Table S3: Loading the indole onto graphene oxide at different concentrations of indole and pH 5.

Item	Primary drug concentration (mol/L)	Primary UV absorption of drug solution (λ)	Final UV absorption of drug solution (λ)	Drug loading efficiency (%)	Quantity of drug loading (%)
1	0	0	0	0.00	0
2	0.02	0.12	0	100.00	48.38
3	0.04	0.2	0	100.00	65.21
4	0.06	0.29	0	100.00	73.76
5	0.08	0.41	0.10	75.61	73.64
6	0.10	0.48	0.20	58.33	73.51
7	0.15	0.73	0.39	46.58	76.76

Table S4: Loading the indole onto graphene oxide at different concentrations of indole and pH 7.

Item	Primary drug concentration (mol/L)	Primary UV absorption of drug solution (λ)	Final UV absorption of drug solution (λ)	Drug loading efficiency (%)	Quantity of drug loading (%)
1	0	0	0	0.00	0
2	0.02	0.12	0	100.00	48.38
3	0.04	0.2	0	100.00	65.21
4	0.06	0.29	0	100.00	73.76
5	0.08	0.41	0	100.00	78.94
6	0.10	0.48	0.620	87.08	80.73
7	0.15	0.73	0.24	67.12	82.57

Table S5: Loading the indole onto graphene oxide at different concentrations of indole and pH 9.

Item	Primary drug concentration (mol/L)	Primary UV absorption of drug solution (λ)	Final UV absorption of drug solution (λ)	Drug loading efficiency (%)	Quantity of drug loading (%)
1	0	0	0	0.00	0
2	0.02	0.12	0	100.00	48.38
3	0.04	0.2	0	100.00	65.21
4	0.06	0.29	0	100.00	73.76
5	0.08	0.41	0.50	87.80	76.59
6	0.10	0.48	0.15	68.65	76.49
7	0.15	0.73	0.41	43.84	75.68

Table S6: Loading the indole onto graphene oxide at different concentrations of indole and pH 11.

Item	Primary drug concentration (mol/L)	Primary UV absorption of drug solution (λ)	Final UV absorption of drug solution (λ)	Drug loading efficiency (%)	Quantity of drug loading (%)
1	0	0	0	0.00	0
2	0.02	0.12	0	100.00	48.38
3	0.04	0.2	0	100.00	65.21
4	0.06	0.29	0	100.00	73.76
5	0.08	0.41	0.31	24.39	44.03
6	0.10	0.48	0.41	21.85	43.46
7	0.15	0.73	0.51	18.14	68.32

Table S7 and Figure S5 indicate the effect of ambient pH on the drug loading efficiency at 0.1 M drug. The drug loading efficiency gradually increased at pHs up to 7 and then decreased. In this respect, the amount of drug absorbed on GO reached maximum at the neutral pH probably due to the free paired-electron on the nitrogen atom in the indole, which could easily form a hydrogen bond with GO. At acidic pHs, however, the surface of indole's nitrogen becomes positive because of protonation. At basic pHs, the surface of indole's nitrogen is deprotonated, and the tendency to bind with the functional group on GO surface gets lower due to the involvement of the free paired electrons. The optimal pH for loading the drug should be therefore neutral.

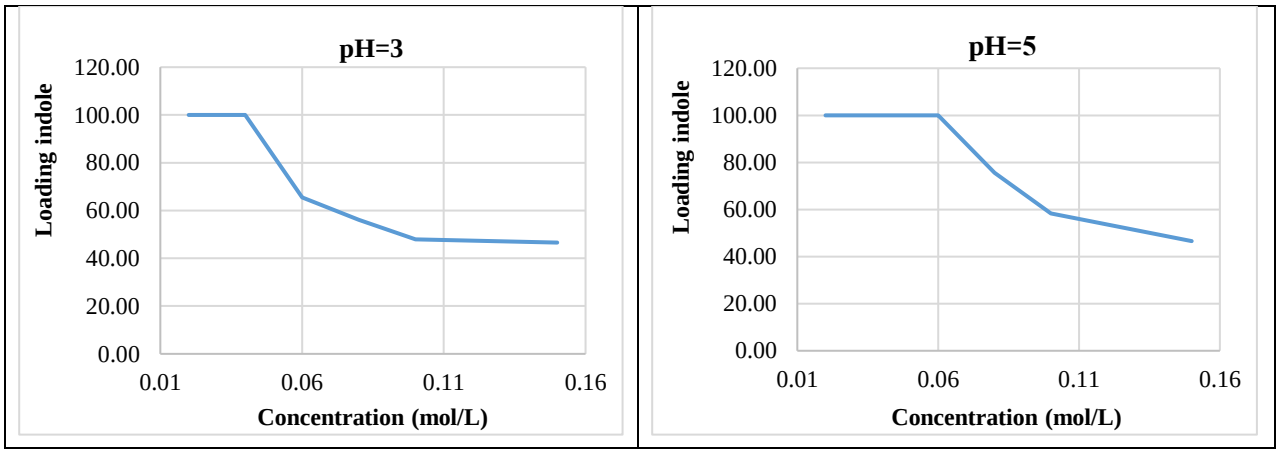

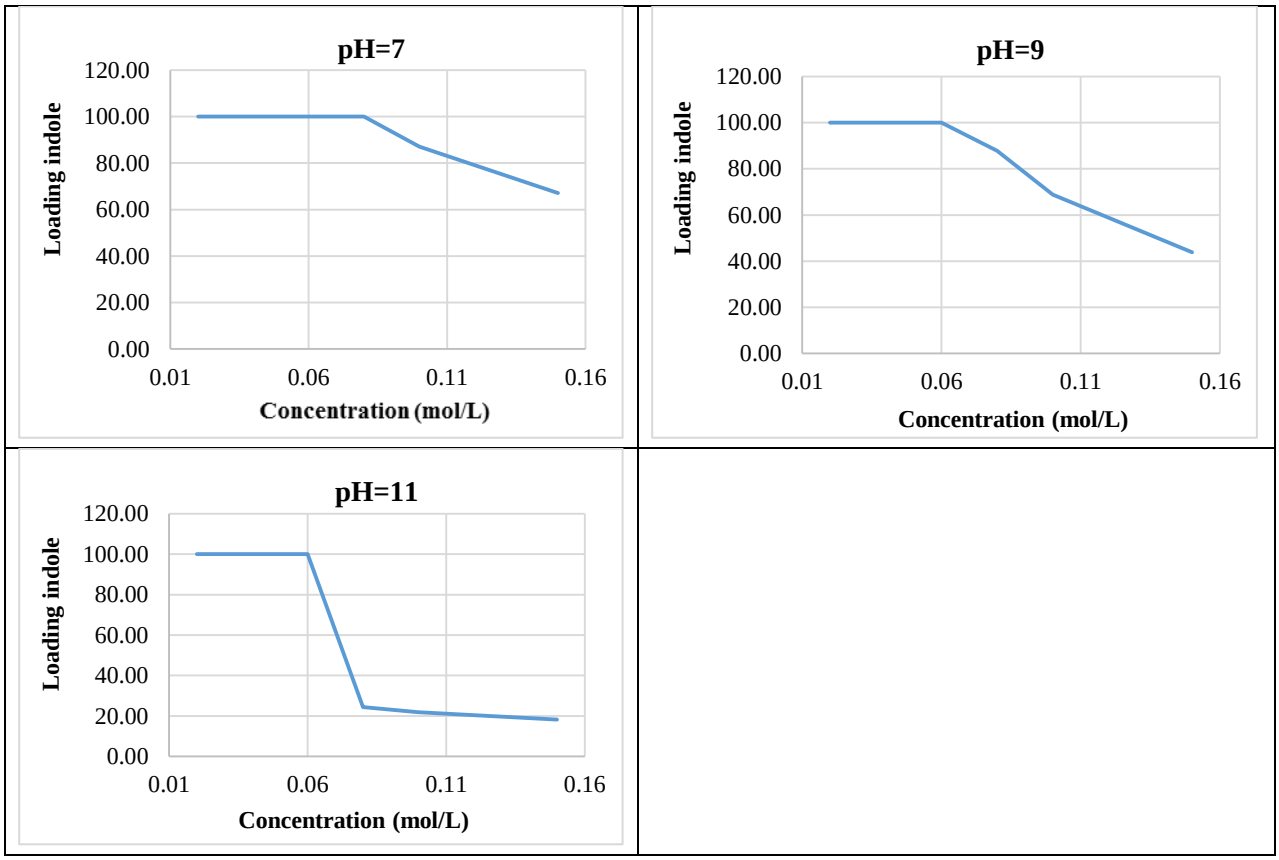

Figure S5a-S5e: Loading the indole onto graphene oxide at different concentrations of indole and pH 3-11

Table S7: The efficiency of loading the indole onto graphene oxide at different pHs and drug concentration of 0.1 M

pH	Percentage of adsorbed drug (Drug loading efficiency) (%)	Percentage of unabsorbed drug (%)
3	47.92	52.08
5	58.33	41.67
7	87.08	12.92
9	68.65	31.35
11	21.85	85.42

Analysis of adsorption isotherm of the drug on graphene oxide

The adsorption isotherm refers to the relationship between variations in adsorption (loading) and the equilibrium concentration of the residual species in solution. There are different types of isotherm that are used to determine the mechanism of the species adsorption process. In this study, Langmuir adsorption isotherm was used to evaluate the adsorption capability and variations in adsorption capacity of the drug on the GO surface at different pHs. In this model, the maximum adsorption happens when the adsorbent surface is totally covered

by a given species. The Langmuir model involves four suppositions as follows: A) The surface of the solid adsorbent is homogeneous, i.e., it contains only one type of material, and there are certain few sites on the adsorbent; B) Each site adsorbs only one molecule, and monolayer adsorption happens under such conditions; C) The adsorbed molecules behave ideally and have no interaction with one another; D) The adsorption process occurs under equilibrium conditions. The following Langmuir equation for the monolayer adsorption is provided [1].

$$\frac{C_e}{q_e} = \frac{C_e}{q_{max}} + \frac{1}{bq_{max}}$$

where, qe is the amount of adsorbent capacity at equilibrium in mg/g; and Ce is the equilibrium concentration in mol/L; q_{max} is the maximum capacity of the monolayer adsorption; b is the Langmuir constant (relevant to the adsorption process energy). The results of all analyses are provided. The amount of R^2 exceeded 0.95 at all pHs, except pH 3, and was thus well conformed to the Langmuir isotherm model.

Table S8: Constants obtained for Langmuir equation

pH	qm (mol.g-1)	b	R^2
3	0.138	8.26	0.8819
5	0.139	366.3	0.9887
7	0.203	109.4	0.9981
9	0.131	1736	0.9997
11	0.052	260	0.9515

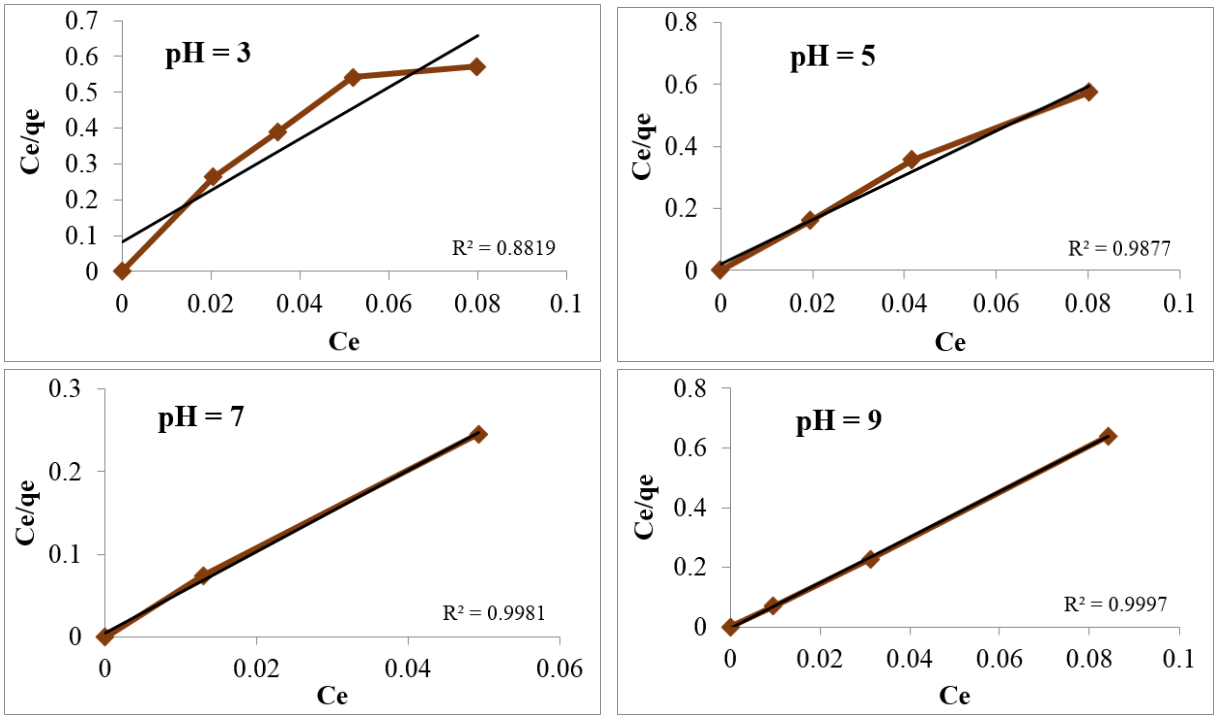

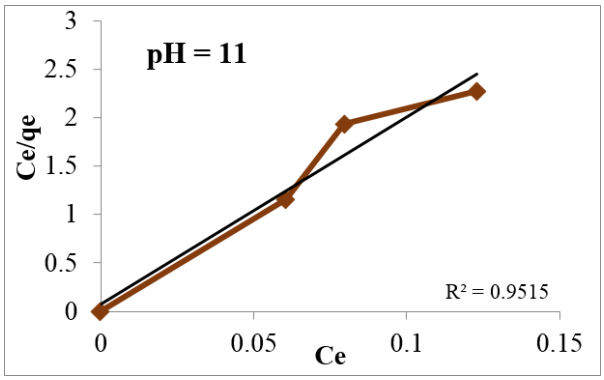

Figure S6. The curve for adsorption of indole in GO nanocarriers.

Analysis of the nanocarriers prepared under ambient storage conditions

To keep the quality of the carriers prepared over time under ambient storage conditions, the release system was analyzed after 1, 7, 14, 30, and 60 days of storage under ambient conditions. Based on the observations, the characteristic peak did not change, and the drug release behavior was the same in a way that the release rate in all the above-mentioned cases at pH 7 reached maximum after 80 minutes, and no change was observed in the UV absorption rate afterwards. The results revealed that the system kept its release profile over the storage time, and the UV absorption of the loaded drug remained stable.

References

1. Liu J, Cui L, Losic D. Graphene and graphene oxide as new nanocarriers for drug delivery applications. Acta biomaterialia. 2013;9(12):9243-57.